SOLAR SUBMILLIMETER AND MILLIMETER SPECTROSCOPY BETWEEN 7 AND 30 cm^{-1} FROM THE JAMES CLERK MAXWELL TELESCOPE

D. A. NAYLOR and G. J. TOMPKINS
Department of Physics, University of Lethbridge, Lethbridge, Alberta T1K 3M4, Canada
T. A. CLARK
Physics Department, University of Calgary, Calgary, Alberta T2N 1N4, Canada
G. R. DAVIS
University of Saskatchewan, Saskatoon, Saskatchewan S7N 0W0, Canada
and
W. D. DUNCAN
Joint Astronomy Centre, University Park, Hilo, HI 96720, U.S.A.

Abstract. A two-beam Martin-Puplett polarizing interferometer has been used in the rapid-scan mode on the 15 meter JCMT in conjunction with the facility detector, UKT14, to survey the solar sub-millimeter and millimeter spectrum in the four wavebands at 7–11, 11–15, 21–24 and 27–30 cm^{-1} to a spectral resolution of 0.01 cm^{-1} and at spatial resolutions of 19″, 16″, 7″ and 6″, respectively. Overall atmospheric transmission through these windows has been evaluated by comparison with synthetic spectra generated with FASCOD/HITRAN. A search has been made for contributions to these spectra from high-n transitions of H and heavier elements by several methods, including the comparison of solar with lunar and limb with disk center spectra.

Key words: infrared: stars – instrumentation: interferometric – Sun: radio radiation

1. Introduction

Solar spectra have been measured through the sub-millimeter and millimeter atmospheric windows from Mauna Kea under dry conditions in February 1991 with a 2-beam polarizing spectrometer mounted on the James Clerk Maxwell Telescope (JCMT). These spectra have been analyzed to evaluate the influence of both the telescope-detector system and variable atmospheric transmission upon the overall quality of such data and to explore the possibility of detecting and observing high-n recombination lines of strength 1% or less. Measurement of the intensities of these lines, extending the measurements already made, from space by *ATMOS* (Farmer and Norton 1989), from the ground in the near IR at 12 μm (*eg.*, Brault and Noyes 1983) and from balloon altitudes in the far IR (Boreiko and Clark 1986), will provide further verification of the modeling of their source regions (see Rutten and Carlsson 1993, and Avrett, Chang and Loeser 1993, in this volume).

2. Instrumentation, Observations and Data Processing

The present data were obtained on February 27, 1991 with a Martin-Puplett polarizing interferometer (Martin and Puplett 1970) mounted at the Nasmyth $f/35$ focus of the JCMT in the double-input port, single output port mode. UKT14, the broad-band bolometric detector (Duncan *et al.* 1990) operating at 0.36 K was used at the output port, with wide-band filters to define the sub-millimeter and

D. M. Rabin et al. (eds.), Infrared Solar Physics, 371–376.

millimeter windows at 350, 450, 850 and 1,100 μm. Focal plane apertures between 21 and 65 mm were selected to match the 6″–19″ range in diffraction beam-widths of the telescope over these wavelengths. In practice, this beam pattern was modified to a greater or lesser extent, depending on wavelength, by the small amplitude but significant beam-pattern extension detected by solar limb scanning (Lindsey and Roellig 1991, Clark *et al.* 1992). The spectrometer uses a metal-grid polarizer/analyzer and beam-splitters on thin Mylar substrates. With the narrow $f/35$ beam of the JCMT Nasmyth focus, it was possible to achieve the design resolution of 0.01 cm^{-1} with no collimation in the spectrometer.

This instrument provides several significant advantages over the conventional IR Michelson interferometer. Modulation efficiency of the metal-grid beamsplitter is constant and much higher over a wide wavelength range than that of thin-film beamsplitters. The complete separation of radiation from the two input ports removes uncertainty about the source of signal modulation.

The highest quality data was obtained in the "rapid-scan" staring mode with an ambient temperature black-body reference source in the second input beam and the telescope secondary mirror held stationary while the scanning roof-top mirror was moved through a complete scan in 45 s. Sets of 10 spectra were taken alternately, on Sun center and on a point 2,000″ from Sun center (or about one solar radius outside of the solar limb) at the same air mass. Spectra were also taken in a slow-scan mode by chopping the JCMT secondary mirror 120″ across the solar limb, using synchronous rectification to take the difference signal and remove atmospheric emission fluctuations during the 15 to 40 minute scans. These data proved to be significantly inferior in quality and resolution to those taken in the rapid-scan mode.

Data analysis followed standard procedure for Fourier transform spectroscopy and used a linear phase correction, since there was little dispersion in the optical elements of the instrument at these wavelengths.

3. Synthetic Spectra

The synthetic spectra used for comparison with the measured spectra were derived from the multi-layer FASCOD2 program (Clough *et al.* 1981), using the HITRAN database (Rothman *et al.* 1987) and the 1976 US Standard Atmosphere for the season and latitude of these observations. This synthesis included the major absorbers H_2O, O_2, O_3, N_2O, CO, CO_2 and CH_4 and the FASCOD continuum absorption term discussed by Clough *et al.* (1981), which contributes significant opacity at these wavelengths. Since the major absorber, H_2O, is usually highly variable, the amount of this constituent was derived from measurements of atmospheric opacity at 225 GHz, (monitored continuously at the Caltech Submillimeter Observatory (CSO), located adjacent to the JCMT) and incorporated into the synthesis. In practice, the atmosphere was found to be remarkably stable through the run and was estimated to contain 0.3 mm of precipitable water vapor. The final synthetic spectrum also incorporated the expected shape of the solar continuum, the UKT14 filter transmissions to low resolution and the airmass relevant to each spectrum.

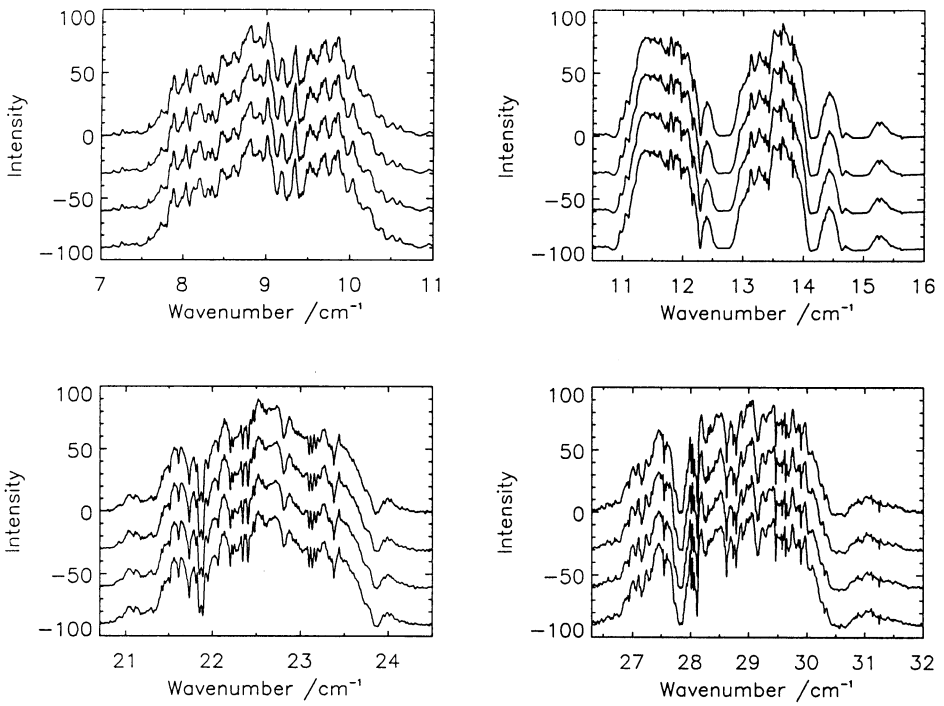

Fig. 1. Sets of 4 individual spectra through the 4 windows at 9, 12.5, 22.5 and 29 cm^{-1}.

4. Discussion of the Spectra

Representative sets of 4 individual sequential spectra at each wavelength, centered upon 9, 12.5, 22.5 and 29 cm^{-1} (270, 375, 675 and 870 GHz, respectively), each taken in 45 s, are shown in Figure 1. These spectra demonstrate excellent repeatability all wavelengths, with the greatest variability in the lowest-transmission, 29 cm^{-1} window, as expected. Overall noise estimates for the instrument in this configuration, (S/N between 80 and 1,000) agree very well with the noise equivalent flux density quoted for UKT14 for wide-band photometry on the JCMT. This indicates that the instrument added no significant noise to the spectra and that the atmospheric transmission fluctuations were small during this period of very dry atmospheric conditions above Mauna Kea.

Figure 2 compares the mean of each set of spectra to its respective synthetic spectrum, generated as described above, and to an equivalent black-body calibration spectrum from ambient-temperature and liquid-nitrogen-cooled cones in the two beams of the interferometer. The synthesis is a good fit to the measured atmospheric transmission in the 26–31 cm^{-1} and 20–25 cm^{-1} intervals, with narrow O_3 lines playing a significant role. A major feature of the 11–16 and the 7–11 cm^{-1}

https://doi.org/10.1017/S0074180900124647 Published online by Cambridge University Press

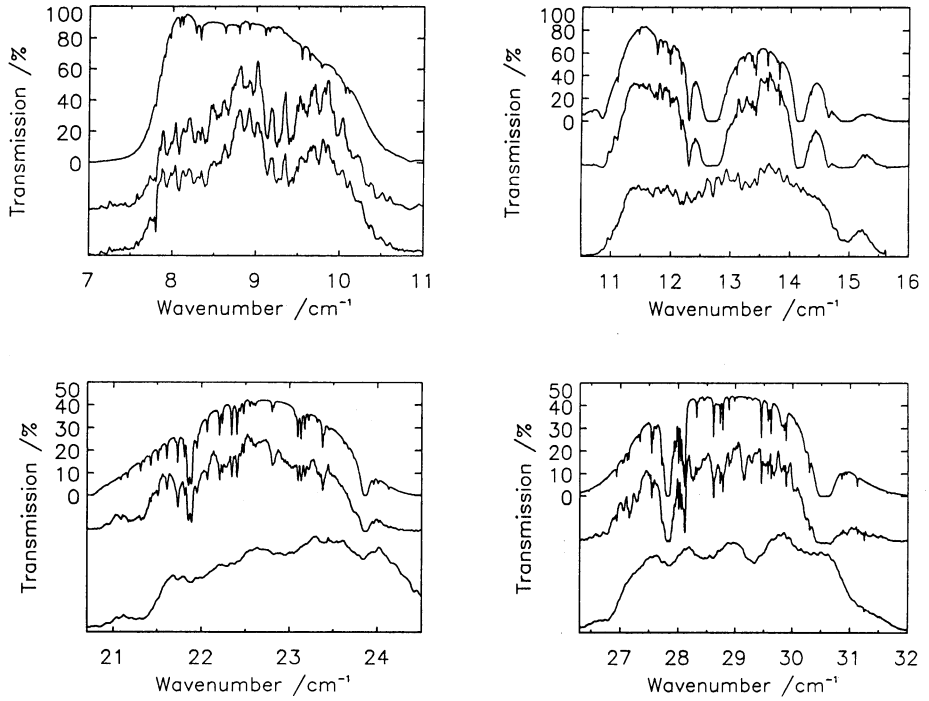

Fig. 2. Comparison of average solar spectra (middle trace) with normalized synthetic transmission spectra (top trace) and calibration spectra (bottom trace) in the 4 windows.

spectra is the rapidly varying structure on the continuum which, since it is reproduced in the calibration spectra, is thought to originate from detector, probably as a result of inadvertent optical cavities within the UKT14 cryostat. This "channel fringe" structure, large enough to mask all but the deepest O_3 lines in the 7–11 cm^{-1} interval, appears to have several characteristic "frequencies" and is fairly close to that in the calibration spectrum. This is not true, however, in the 20–25 and 26–31 cm^{-1} intervals, where the calibration spectra show slowly varying fluctuations with wavenumber and not the more rapid changes apparent in the solar and lunar spectra. It is also apparent in this comparison that the shape of the measured spectral envelope is dominated by the wings of the strong H_2O lines and that this shape will be very dependent upon airmass. This in turn means that calibration sources should be measured at very similar air masses wherever possible to avoid errors in the correction for atmospheric transmission shape. The Moon is a suitable calibration source for these solar measurements, but its position is rarely ideal, and the low overall signal and variations in emission across its surface may provide less than ideal calibration.

https://doi.org/10.1017/S0074180900124647 Published online by Cambridge University Press

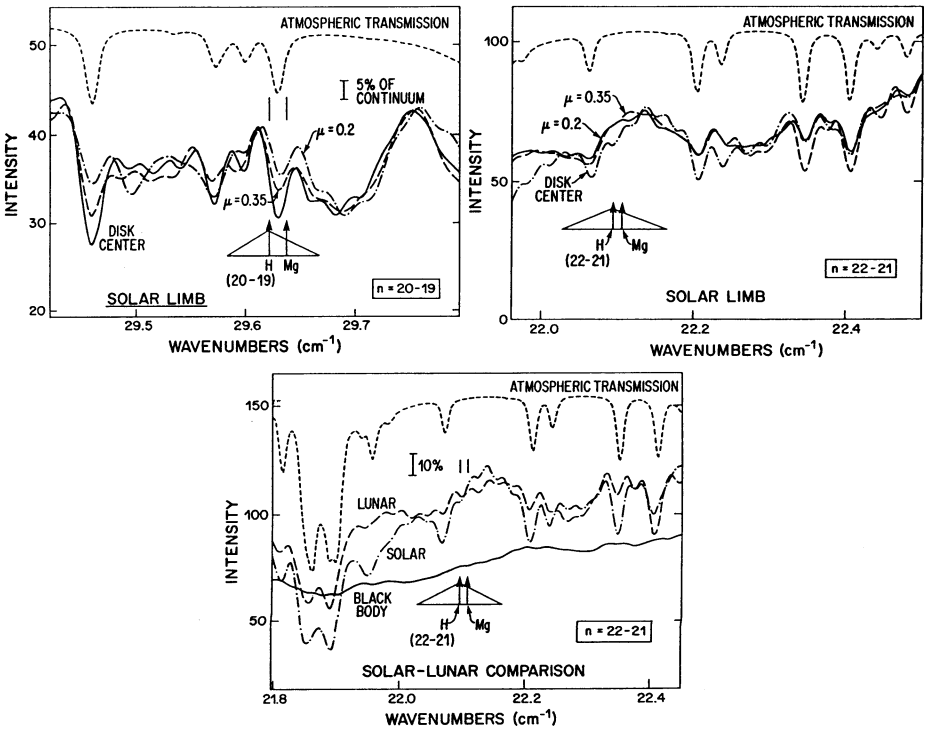

Fig. 3. (a) and (b) Comparison of normalized sections of spectra around the $n = 20$–19 and 22–21 recombination line positions at 29.622 and 22.095 cm^{-1} at disk center and at $\mu = 0.35$ and 0.2 and (c) comparison of solar and lunar spectra at 22.095 cm^{-1}, along with the calculated atmospheric transmission.

5. Line Search

Several techniques were used in this initial search for high-n solar emission lines with the polarizing interferometer. Rapid-scan spectra at solar disk center were compared to lunar spectra from another time and airmass. Slow-scan spectra were taken in 2 positions, chopping the secondary mirror 120″ across the solar limb. The first was taken with one beam 60″ inside the limb ($\mu = 0.35$), and the second only 20″ inside the limb ($\mu = 0.20$) to utilize any limb brightening effects. Spectral quality, was significantly poorer in the slow-scan spectra, probably due to atmospheric transmission fluctuations over the scan time. Figure 3 shows normalized spectra near expected line positions to compare the solar-disk-center and lunar spectra, and solar-limb and disk-center spectra, for $n = 20$–19 and 22–21. Continuum intensity and line widths predicted by Hoang-Binh (1982), are shown for each line. There is little evidence of excess emission at these positions. Better calibration with reduced channel-fringe structure will be needed in future searches.

https://doi.org/10.1017/S0074180900124647 Published online by Cambridge University Press

6. Conclusions

The present spectra of the Sun show excellent reproducibility and signal-to-noise, but contain significant structure due to detector "sensitivity" variations across the filter band-passes, which appear to be beam-width dependent and somewhat difficult to calibrate out at the present time. Determination of the instrumental transmission function using both ambient-temperature and cooled black-body cones in the two beams of the Martin-Puplett interferometer is shown to reproduce the general overall shape at the longer wavelengths but provides only a hint of the rapid fluctuations in instrument function seen in the solar and lunar spectra at the shorter wavelengths, perhaps because of different input beam geometry into the detector optics. This structure, without adequate calibration, makes it difficult to identify weak, relatively broad line features such as the expected emission lines from high-n states of H and other elements. Modification of the optical system of UKT14 to remove the major cavity effects has already been accomplished but is unlikely to eliminate these effects completely. The calibration of spectra from the Sun, planets and other sources will pose difficulties, in view of the requirement for beam-width matching, particularly in the accurate representation of the continuum envelopes of sources.

Acknowledgements

It is a pleasure to thank the staff of the James Clerk Maxwell Telescope for their efforts in mounting the interferometer and in supporting these experiments. This telescope is operated by the Royal Observatory Edinburgh on behalf of the Science and Engineering Research Council of the United Kingdom, the Netherlands Organization for Scientific Research and the National Research Council of Canada. This work has been supported by NSERC and NRC of Canada research and travel grants and this support is gratefully acknowledged.

References

Avrett, E. H., Chang, E. S. and Loeser, R.: 1993, these proceedings.
Boreiko, R.T. and Clark, T.A.: 1986, *Astron. Astrophys.*, **157**, 353.
Brault, J.W. and Noyes, R.W.: 1983, *Astrophys. J. (Letters)*, **269**, L61.
Clark, T.A., Naylor, D.A., Tompkins, J.G. and Duncan, W.D.: 1993, *Solar Phys.*, in press.
Clough, S.A., Kneisys, F.X., Rothman, L.S., Gallery, W.O.: 1981, *SPIE*, **277**, 152.
Duncan, W.D., Robson, E.I., Ade, P.A.R., Griffin, M.J. and Sandell, G.: 1990, *Mon. Not. Roy. Astron. Soc.*, **243**, 126.
Farmer, C.B. and Norton, R.H.: 1989, *A High Resolution Atlas of the Infrared Spectrum of the Sun and the Earth Atmosphere from Space*, Vol. I: The Sun, NASA Ref. Pub. 1224, Washington, D.C.
Hoang-Binh, D.: 1982, *Astron. Astrophys.*, **112**, L3.
Lindsey, C.A. and Roellig, T.L.: 1991, *Astrophys. J.*, **375**, 414.
Martin, D.H. and Puplett, E.F.: 1970, *Infrared Phys.*, **10**, 105.
Rothman, L.S., Gramache, R. R., Goldman, A., Brown, L. R., Toth, R. A., Pickett, H. M., Poynter, R. L., Flaud, J.-M., Camy-Peyret, C., Barbe, A., Husson, N., Rinsland, C. P. and Smith, M. A. H.: 1987, *Applied Opt.*, **26**, 4058.